Available online at www.sciencedirect.com
SCIENCE DIRECT®
International Journal of Coal Geology 59 (2004) 193–208
International Journal of COAL GEOLOGY
www.elsevier.com/locate/ijcoalgeo

Modes of occurrence of mercury and other trace elements in coals from the warrior field, Black Warrior Basin, Northwestern Alabama

S.F. Diehl*, M.B. Goldhaber, J.R. Hatch

U.S. Geological Survey, Box 25046, Denver, CO 80225, USA

Received 28 January 2004; received in revised form 17 February 2004; accepted 17 February 2004
Available online 27 April 2004

Abstract

The mineralogic residence and abundance of trace metals is an important environmental issue. Data from the USGS coal quality database show that potentially toxic elements, including Hg, As, Mo, Se, Cu, and Tl are enriched in a subset of coal samples in the Black Warrior Basin of Alabama, USA. Although the coal as-mined typically is low in these elements, localized enrichments occur in high-pyrite coals and near faults. Microscopic analyses demonstrate that the residence of these elements is dominantly in a late-stage pyrite associated with structurally disrupted coal. Further, our data suggest addition of Hg to the coal matrix as well. The source of these trace elements was hydrothermal fluids driven into the Black Warrior Basin by Alleghanian age tectonism. Published by Elsevier B.V.

Keywords: Coal; Mercury; Arsenic; Black Warrior Basin; Pyrite

1. Introduction

Coal combustion is a significant source of Hg to the environment (Kolker et al., 1999; Finkelman et al., 2002; Sakulpitakphon et al., 2004). According to 1994 data from the U.S. Environmental Protection Agency (EPA) (1997), emissions from coal combustion account for about 34% of the Hg released to the atmosphere (US EPA, 1997). Understanding the controls on the abundance and mineralogic residence of Hg in coal can aid in evaluating the potential for environmental impacts from the coal production–utilization cycle. This study focuses on Hg occurrences in coal in the Warrior field, Black Warrior Basin, northwestern Alabama. Based on a USGS database of coal analyses, the Warrior field coal has locally elevated Hg levels, as well as elevated contents of As, Mo, Se, Cu, and Tl (Goldhaber et al., 2000). Of these element enrichments, As content is by far the highest. On a basin scale, As and Hg tend to be co-located (Goldhaber et al., 2000).

Microanalysis of coal samples from three coalmines in the Warrior field shows that As is dominantly concentrated in the sulfide mineral pyrite (FeS_2; Kolker et al., 1999; Diehl et al., 2002). Milling and waste disposal processes have concentrated pyrite in

* Corresponding author. Tel.: +1-303-236-1830; fax: +1-303-236-1425.
E-mail addresses: diehl@usgs.gov (S.F. Diehl), mgold@usgs.gov (M.B. Goldhaber), jrhatch@usgs.gov (J.R. Hatch).

0166-5162/$ - see front matter. Published by Elsevier B.V.
doi:10.1016/j.coal.2004.02.003

waste piles; weathering has released this As, which has accumulated in the environment. Goldhaber et al. (2000) reanalyzed stream sediment samples, collected from 3000 sites in northern Alabama during the National Uranium Resource Evaluation (NURE) (Smith, 2001) program in the early 1970s, for a suite of trace metals. Stream sediments from coal mining areas were determined to be elevated in As compared to adjacent areas (Goldhaber et al., 2000). These previous microscopic and stream sediment studies did not focus on the details of the Hg distribution, its relation to As, its occurrence as a function of pyrite grain size or paragenesis, nor did they examine the possibility that Hg may occur at significant concentration levels in the organic components of the coal. These issues are important because relatively coarse-grained pyrite can be removed from coal, decreasing the content of pyrite-associated elements during combustion, whereas fine-grained pyrite and the coal itself are less amenable to cleaning. In addition, coal utilization may contribute substantial amounts of these elements to the environment by processes other than combustion. Pyrite-rich coalmine wastes were deposited in or near drainages during an earlier era of mining. Oxidation of this pyrite may release trace elements from mine waste or abandoned coalfaces into surface or ground waters (Goldhaber et al., 2002).

In this study, we use microanalytical techniques to determine trace metal associations and relative timing of trace metal influx. We demonstrate that Hg, As and other trace elements were emplaced late in a sequence of multiple deformation events and concurrent pyrite precipitation in structurally disrupted coals in the Warrior field, and that Hg may also be added to the organic coal matrix itself.

2. Geologic setting

The triangular-shaped Black Warrior Basin is a major structural feature in northern Alabama (Fig. 1). The basin formed by the convergence of the Ouachita and Appalachian thrust belts in Late Paleozoic time. The basin is bounded on the southeast by the Appalachian orogen, southwest by the Ouachita orogen, and to the north by the Nashville Dome. The basin adjoins the northeast–southwest trending Appalachian Basin (Pashin, 1991). A major thrust fault system of the Alleghanian orogeny borders the Black Warrior Basin on the southeast. This thrust fault system generated folds with northeast–southwest trending axes (Fig. 1) that separate the Black Warrior Basin from metamorphosed rocks further to the southeast. The Cahaba and Coosa coal fields lie within this fold belt (Fig. 1).

Normal faults and graben systems in the Black Warrior Basin trend northwest–southeast, perpendicular to the fold axis trends (Pashin, 1991; Pashin et al., 1999). The normal faults can be extensive, up to 15-km in length, and are recorded at all scales in the rock, from kilometer-scale structures to mm-scale structures. These faults were likely pathways for the migration of metal-bearing solutions that were mobilized during the Alleghanian orogeny (Goldhaber et al., 2000). Coals adjacent to the normal faults are mineralized at all scales by sulfide and (or) carbonate minerals (Goldhaber et al., 2002).

In the Warrior field, coal occurs in the Pottsville Formation of lower Pennsylvanian age. The Pottsville Formation is overlain unconformably by Cretaceous and younger rocks of the Mississippian Embayment and Gulf Coastal Plain. The lower part of the Pottsville Formation consists primarily of quartzose sandstone with thin discontinuous coals. The upper part of the Pottsville Formation contains seven major and three minor coal zones that cap regressive cycles, which coarsen upward from mudstone to sandstone (Pashin, 1991). Stratigraphically, from oldest to youngest, these major zones are the Black Creek, Mary Lee, Pratt, Cobb, Gwin, Utley, and Brookwood zones (Culbertson, 1964; Pashin, 1991). The coals contain thin to thick vitrain (bright, black, brittle, and fractured) and clarain (semi-brittle, black, finely stratified) bands (Goldhaber et al., 2000).

3. Trace elements in warrior field coals

Contents of Hg, As and other potentially hazardous elements [e.g., Sb, Mo, Tl) are locally elevated in coals of the Warrior field of Alabama (Fig. 2; Table 1) (Oman et al., 1995; Goldhaber et al., 1997, 2000; Kolker et al., 1999; Hatch et al., 2001). Bragg et al. (1997) show that for nearly 960 samples, the average (mean) content of As in Alabama coal (72 ppm) is three times higher than the average for all US coal (24

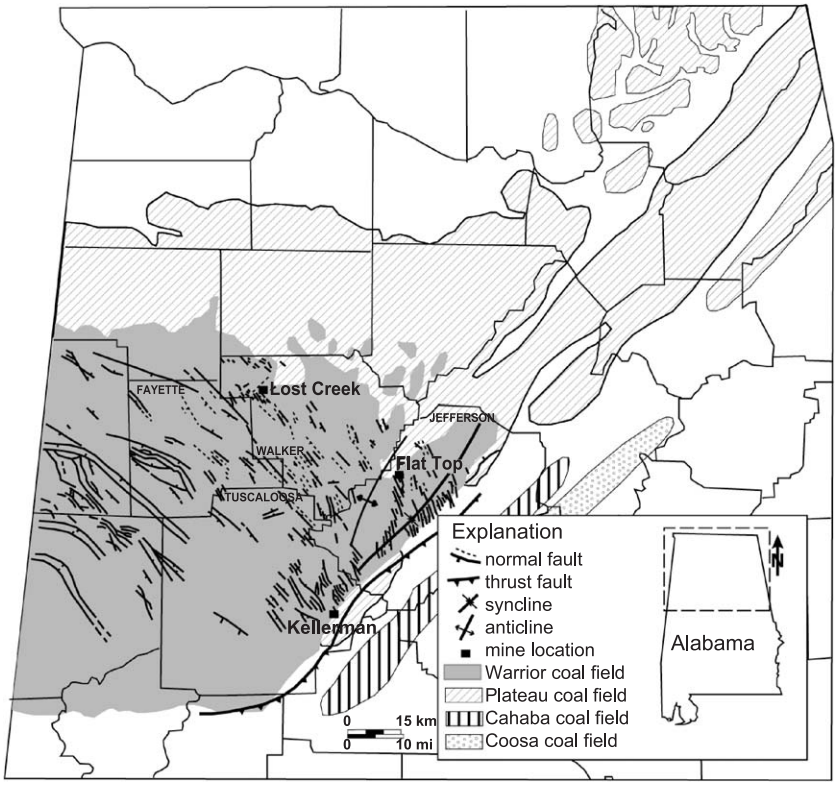

Fig. 1. Map of northern Alabama, depicting the location of Lost Creek, Kellerman, and Flat Top mines, an Alleghanian thrust fault, axes of folds, and a strong northwest to southeast trending normal fault system (after Pashin, 1991). The latter fault system was a probable fluid migration pathway for metal-bearing solutions.

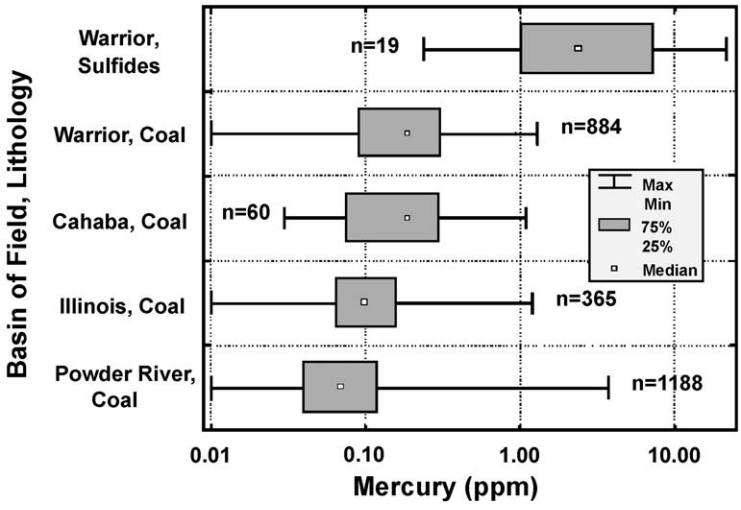

Fig. 2. Plot illustrating medians, ranges anf the 75 percentiles for Hg contents in Warrior field sulfides and Warrior field, Cahaba field, Illinois Basin and Powder River Basin coals, USA [Mercury content in sulfide minerals (data from this study) was summarized separately to show that Hg is predominantly contained within the mineral pyrite, n = number of samples].

Table 1
Statistical summaries of mercury contents in Warrior field sulfides and Warrior field, Cahaba field, Illinois Basin and Powder River Basin coals, USA

Basin or field, Lithology	*n*	Hg median (ppm)	Hg range (ppm)	25th percentile (ppm)	75th percentile (ppm)
Warrior field, Sulfides	19	2.40	0.24–21.6	1.00	7.50
Warrior field, Coal	884	0.19	0.01–1.3	0.09	0.31
Cahaba field, Coal	60	0.19	0.03–1.1	0.08	0.31
Illinois Basin, Coal	365	0.10	0.01–1.2	0.06	0.16
Powder River Basin, Coal	1188	0.07	0.01–3.8	0.04	0.12

Warrior field and Powder River Basin coal data are from Bragg et al. (1997). Illinois Basin summaries are from Affolter and Hatch (2002) and represent data from the Springfield, Herrin, Danville, and Baker Coals. Warrior field sulfides and Cahaba field coal data are summarized from unpublished data of J.R. Hatch and M.L. Goldhaber. *n* = number of samples.

ppm). Of the US coal analyses for As that are at least three standard deviations above the mean, approximately 90% are from the coal fields of Alabama. Selenium, Mo, Sb, and Cu are also enriched in Warrior field coals compared to national averages (Goldhaber et al., 2000). The median content of Hg in coals from both the Warrior field (0.19 ppm) and adjacent Cahaba field (0.19 ppm) exceed those of the Illinois Basin (0.10 ppm) and the Powder River Basin (0.07 ppm) (Fig. 2; Table 1).

The overall spatial and stratigraphic distribution of trace elements and sulfide S in Warrior field coals has previously been described (Goldhaber et al., 2000). Elevated As contents, well above the average for all US coal (24 ppm—see above), are present in all of the coal zones. There is also an apparent tendency for the highest values to cluster in the lower coal zones (Black Creek, Mary Lee, and Pratt) (Goldhaber et al., 2000). High contents of As are not uniformly distributed throughout the Warrior field. Instead, high contents are consistently present in northern Tuscaloosa, eastern Fayette, and western and eastern Walker Counties (Fig. 1). Generally, the areas with high Hg contents coincide geographically with high As areas. It does appear that relative to As, Hg is concentrated in the upper coal zones (Cobb and Utley, and Brookwood). These relatively elevated Hg contents prompted this study of the distribution of this element in samples of Warrior field coals.

4. Methods

For this study of trace-element modes of occurrence, we analyzed coal samples containing pyrite from the Lost Creek, Flat Top, and Kellerman mines in the Warrior coal field (Fig. 1; Table 2). These samples are described in Table 2. As the table shows, field sampling was focused on comparison of coal compositions within and near fault zones, to coal away from fault zones.

Polished samples of the coal were examined using petrographic and microanalytical techniques (Vassilev and Tascón, 2003). Reflected light microscopy and scanning electron microscopy with energy dispersive X-ray spectrometer (SEM/EDS) were used to determine basic mineralogy, to analyze structural features, and for qualitative analysis of trace-element content and distribution in sulfide minerals (Huggins, 2002; Ward, 2002). Digital element maps and line scans were obtained on a JEOL JXA-8900 electron probe

Table 2
Description of samples

Mine	Sample number	Stratigraphic and geologic setting	Sample characteristics
Lost Creek	NC-3	Newcastle Coal, Mary Lee Group; sulfide lens	pyrite-filled cellular structures (lumens) with crosscutting microfaults and microveins
Flat Top	AM-2	American Coal, Pratt Group; 6–8′ (~ 2 m) from fault	pyrite-filled cellular structures (lumens) with crosscutting microfaults and microveins
Kellerman	2–7	Milldale Coal, Brookwood Group; major fault zone	crosscutting pyrite-filled vein network
	MD-2	Milldale Coal, Brookwood Group 1–2′ (~ 0.5 m) from fault with minor offset	crosscutting pyrite-filled vein network

The Lost Creek and Flat Top surface mines were active, the Kellerman surface mine was abandoned at the time of sample collection.

Table 3
Trace element contents in pyrite determined by laser ablation inductively coupled plasma mass spectrometry (LA-ICP-MS)

Mine; sample no.	Sample description; pyrite morphology	*n*	Zn ppm Average (Range)	Cu ppm Average (Range)	As ppm Average (Range)	Se ppm Average (Range)	Mo ppm Average (Range)	Sb ppm Average (Range)	Au ppm Average (Range)	Hg ppm Average (Range)	Tl ppm Average (Range)	Pb ppm Average (Range)
Lost Creek NC-3	framboids	5	37 (0–70)	5 (4–7)	530 (240–790)	0*	7 (4–11)	0.90 (0–1.44)	0	0	2.7 (2.3–3.1)	4 (3–5)
	cell fill; massive pyrite	4	0	1 (0–3)	38 (0–90)	0	0	0	0	0	0.30 (0.01–1)	0
	cell overgrowth/cell replacement/fracture[a]	6	0	0	8800 (300–17300)	0	0	0	0	0	6 (1–10)	0.06 (0–0.3)
	massive pyrite in vein	35	12 (0–80)	N.A.	4130 (80–27400)	0	9 (0–45)	0.40 (0–2)	0.03 (0–0.2)	17 (7–39)	7 (1–13)	0.70 (0–18)
Flat Top AM-2	vein	21	4 (0–15)	0.7 (0–3)	1320 (101–2484)	66 (7–130)	76 (11–200)	0.55 (0–7)	0.06 (0–0.3)	21 (4–39)	6 (2–9)	0.60 (0.01–9)
	cell fill/pyrite in fusinite layer	31	4 (0–20)	0.2 (0–2)	1860 (597–2208)	286 (37–510)	52 (7–582)	0.11 (0–0.6)	0.90 (0–0.9)	8.3 (0–27)	3.45 (1.90–5.20)	0.60 (0–3)
Kellerman MD-2	massive pyrite in veins	30	20 (0–110)	N.A.	5170 (1075–10530)	0	49 (12–200)	2.1 (0–12)	0.04 (0–0.22)	18 (2–102)	7 (1–33)	2 (0.02–7)
	crosscutting veins/ younger vein set	5	N.A.	0.4 (0–2)	6920 (5780–8700)	195 (150–250)	28 (22–41)	0.80 (0–1)	0	0	19 (15–21)	0.40 (0.2–0.5)
	crosscutting veins/ older vein set	6	N.A.	11 (7–15)	4980 (3920–5740)	280 (130–410)	19 (11–27)	11 (1–48)	0	27 (16–40)	16 (11–22)	0.70 (0.40–1)
	growth-banded massive pyrite in younger vein	3	N.A.	0.3 (0–1)	11200 (10870–11600)	250 (240–255)	43 (40–50)	2.5 (0–6)	0	0	15 (14–15)	0.30 (0.2–0.4)
Kellerman 2–7	framboids	5	30 (0–160)	20 (13–30)	86 (78–95) 0	0	16 (10–25)	76 (11–140)	0	0	0.80 (0.60–1.00)	2 (0.50–7)
	recrystallized framboid near vein	1	0	55	2476	0	23	20	0	0	7	7
	massive pyrite in veins	34	5 (0–20)	4 (0–20)	2700 (23–7500)	76 (4–590)	38 (2–80)	16 (1–51)	0.04 (0–0.20)	20 (5–104)	4 (0.10–8)	0.50 (0.03–4)

n = number of analyses; ppm = parts per million; N.A. = not analyzed.
[a] Microfractures and faults through pyrite-filled cell structures show arsenic-enrichment (see Fig. 9).
* 0 = below detection limit in sample.

microanalyzer (EPMA) to determine the spatial distribution of S, Fe, As, and other associated trace metals. With the exception of As, the concentration of trace metals of interest was too low to map in two dimensions with the microprobe. However, using spot mode, with a 0.5-μm step interval and 2-μm excitation volume, at 15 kv, a probe current of 20 nA (cup), and a dwell time of 5000 ms, EPMA X-ray elemental line scans provided qualitative information on relative Hg abundance. By simultaneously running a scan on a wavelength peak near that of the Hg peak, and later comparing background X-ray counts to counts obtained at the Hg peak, a Hg spectrum was obtained. This made it possible to analyze the Hg line scans and compare Hg concentration to As concentration within pyrite. (Any use of trade names or commercial products is for descriptive purposes only and does not imply endorsement by the US Government.)

We were also able to quantitatively determine the contents of Hg and other minor elements at selected spots in the coal samples with laser ablation inductively coupled plasma mass spectrometry (LA-ICP-MS) (Tables 3 and 4) (Ridley, 2000). LA-ICP-MS analyses were performed on a Perkin-Elmer Sciex Elan 6000 quadrupole mass spectrometer attached to a CETAC LSX200 laser system. Trace element contents are typically much lower in coal than pyrite, requiring a larger beam size to obtain usable data. Therefore, we used a 10- to 25-μm beam diameter for pyrite and a 100- to 200-μm beam diameter for coal. U.S.G.S. sulfide standard PS-1 (Wilson et al., 2002) was used as a calibration standard for pyrite analysis and NIST (National Institute of Standards and Technology) 1632B was used as a standard for coal analysis.

5. Results

5.1. Textural and paragenetic characterization of pyrite

Previous studies showed that pyrite is the dominant residence for the elevated levels of As present in Warrior Basin coal (Kolker et al., 1999; Diehl et al., 2002; Goldhaber et al., 2002). Using LA-ICP-MS, we have been able to show in this study, that pyrite is also the dominant host of a suite of trace elements includ-

Table 4
Trace element contents in coal determined by laser ablation inductively coupled plasma mass spectrometry (LA-ICP-MS data)

Mine sample no.	*n*	S ppm Average (Range)	Ca ppm Average (Range)	Fe ppm Average (Range)	Cu ppm Average (Range)	Zn ppm Average (Range)	As ppm Average (Range)	Mo ppm Average (Range)	Sb^{121} ppm Average (Range)	Hg^{202} ppm Average (Range)	Tl^{205} pm Average (Range)	Pb^{208} ppm Average (Range)
Lost Creek	33	626	73	22	0.58	2	1.95	0.30	0.06	0.18	0.10	0.06
NC-3		(310–1270)	(0–250)	(7–60)	(0–1.8)	(0–7.20)	(0.31–5.28)	(0–0.89)	(0–0.20)	(0.10–0.31)	(0.02–0.57)	(0–0.40)
Flat Top	18	503	24	39	0.37	2	4	1.20	0.12	0.05	0.09	0.84
AM-2		(410–590)	(7–120)	(1.5–180)	(0.01–3)	(0–26)	(0–69)	(0.20–2.40)	(0–1.10)	(0.04–0.08)	(0–0.32)	(0.002 14)
									0.05			
									(0.04–0.08)			
Kellerman	32	700	17	7	0.38	0.48	0.70	0.43	0.02	0.20	0.02	0.04
MD-2		(585–980)	(8–30)	(2–40)	(0.10–1)	(0–2.87)	(0–4.05)	(0.12–0.95)	(0–0.09)	(0.12–0.41)	(0–0.14)	(0–0.60)
Kellerman	29	9230	224	46	5	2	0.50	6	0.42	0.30	0.09	0.08
2–7		(7860–12060)	(71–670)	(120–1360)	(0.40–90)	(0.32–4)	(0–3)	(4–10)	(0.02–1.30)	(0.19–0.43)	(0.01–0.36)	(0.003–0.30)

n = number of analyses; ppm = parts per million.

ing Hg, Mo, Se, Cu, and Tl, contents of which are known to be elevated in whole coal analyses from the basin. The average (mean) concentrations, determined by LA-ICP-MS, of selected trace elements in pyrite and coal are reported in Tables 3 and 4 and plotted in Fig. 3. The contents of Hg, As, Mo, Sb, Tl, and Pb, are, on average, one to three orders of magnitude higher in pyrite than in immediately adjacent coal. Gold was analyzed because the suite of elements enriched in coal is consistent with sediment-hosted Au deposits (Goldhaber et al., 2002). In fact, Au contents in pyrite are elevated by over an order of magnitude above the average crustal Au content of 0.004 ppm. Mercury in pyrite samples examined in this study averages about 10 ppm, but is closer to 0.1 ppm in coal. For this reason, our study focused in part on characterizing the pyrite and the relative timing of trace element enrichment.

Reflected light microscopy and SEM observations show that there are several generations and morphological forms of pyrite in coal samples from the Lost Creek, Flat Top, and Kellerman Mines. In all the samples, the earliest generation of pyrite is framboidal, composed of spherical masses of microcrystalline pyrite cubes. Framboidal spheres are typically ≤ 10 μm in diameter and are randomly scattered in the coal bands. Framboids may be encased in, or overgrown by, later coarse-grained generations of pyrite (Hatch et al., 2001, their Fig. 5; Diehl et al., 2003, their Fig. 8). In the Lost Creek Mine samples, coarse-grained massive pyrite (1) fills woody cell structures, (2) occurs as rims or overgrowths outside the cell wall boundaries, and (3) lines microfaults and microveins that crosscut the cells (Diehl et al., 2002) (Fig. 4). Pyrite in the cell structures is As-poor, but the successive generation of pyrite overgrowths and pyrite in the deformation structures is As-rich (Fig. 4).

Woody cell structures in coal samples from the Flat Top mine are commonly filled by pyrite, but the cells lack the overgrowths recognized in the Lost Creek samples. In addition to pyrite, woody cell structures are filled by calcite, kaolinitic clay, and (or) apatite. Calcite and clay are commonly etched and embayed, indicating partial dissolution within the cells. Remnants of calcite and clay are enclosed by coarse-grained As-rich pyrite, indicating that pyrite is the later phase and post-dated dissolution.

In all the mine samples, deformation features in coal such as microfaults and microveins are filled with pyrite (Figs. 4 and 5). Both macroscopic and microscopic fracture/fault surfaces from the Flat Top Mine coal samples have calcite and pyrite coatings. Pyrite is always the later epigenetic phase. Coal samples collected from faulted coal beds from the Kellerman mine show a dense network of pyrite-filled, crosscutting veins. Veins are multigenerational, spanning an age range from mineral-filled pre-solidification shrinkage-type cracks, to post-solidification brittle deformation fractures in the coal. Veins commonly branch at their tips; they occur as single veins or in

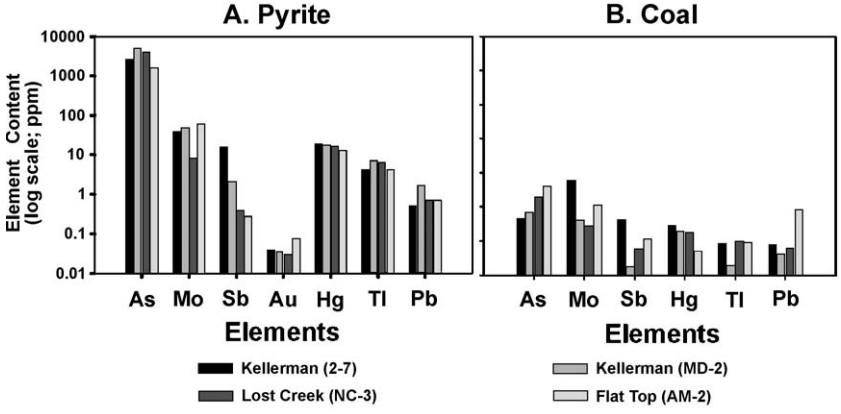

Fig. 3. (A) Plot showing mean contents of selected trace metals in pyrite from Kellerman, Lost Creek, and Flat Top mine samples. (B) Plot showing mean contents of trace metals in coal samples from the Kellerman, Lost Creek, and Flat Top mines. Note that average contents in coal are typically an order-of-magnitude less than average contents in pyrite.

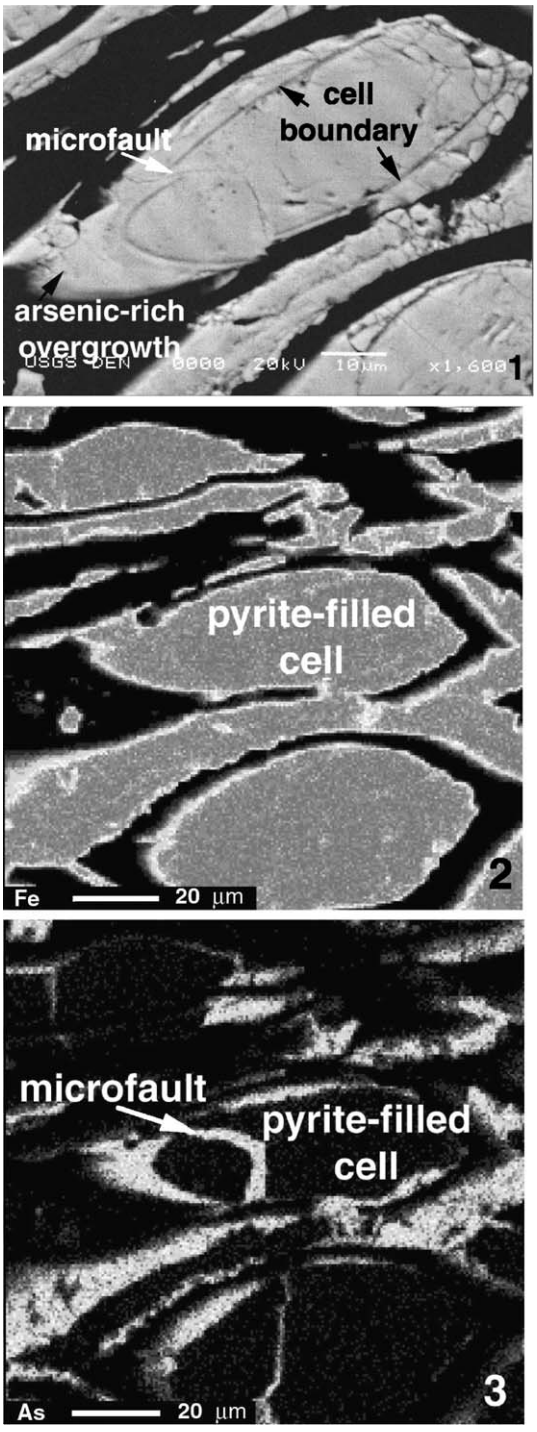

orthogonal sets. A dense network of horizontal and vertical pyrite-filled veins may be crosscut by a later generation of pyrite-filled veins. Veins commonly range from 10- to 100-μm in thickness (Fig. 5). Veins show lateral textural changes, such as from massive to dendritic forms. Textural changes across a vein commonly reflect a change in trace metal content (e.g. Fig. 5b). Late-stage pyrite-filled veins and faults commonly crosscut the pyrite-filled woody cell structures. Because of their enrichment in heavy trace metals, these veins and faults are visible using backscattered electron imaging with SEM or EPMA (Figs. 4 and 5A). This late-stage coarse-grained pyrite that fills deformation structures appears to be temporally related to the last generation of overgrowth of pyrite around cells (Fig. 4).

Arsenic-rich veins commonly show etched, partial dissolution textures due to alteration or weathering. Semi-quantitative SEM-EDX data demonstrates that weathered pyrite remnants in veins are typically depleted in As content. For example, in a sample from the Kellerman mine, the unaltered part of an As-rich vein has a content of 1.2 wt.% As, whereas the dissolution-etched part of the same vein contains 0.4 wt.% As.

5.2. Trace elements in pyrite

Analyses by laser ablation and microprobe studies shows that Hg and As are heterogeneously distributed in a crosscutting vein network (Fig. 5). The veins are made up of several generations of pyrite, as described above. EPMA element distribution maps and line scans of Hg and As across pyrite-filled veins show that trace-metal enrichment occurred preferentially only in certain pyrite generations within the veins (Figs. 4 and 5). The element distribution maps also show that As in pyrite is high enough in concentration (up to 2.7 wt.%; Table 3) to reveal growth-banding textures and to delineate distinct vein generations (see

Fig. 4. From top to bottom, (1) backscatter scanning electron photomicrograph of a pyrite-filled cell structure with an As-rich overgrowth/rim and crosscut by a microfault which offsets the cell boundary (Lost Creek mine); (2) EPMA element map of iron, showing pyrite-filled cells and cell walls, and (3) EPMA element map of As, showing As-poor pyrite in cell structures and As-rich overgrowths/rims as well as As-rich alteration along microfaults and microfractures.

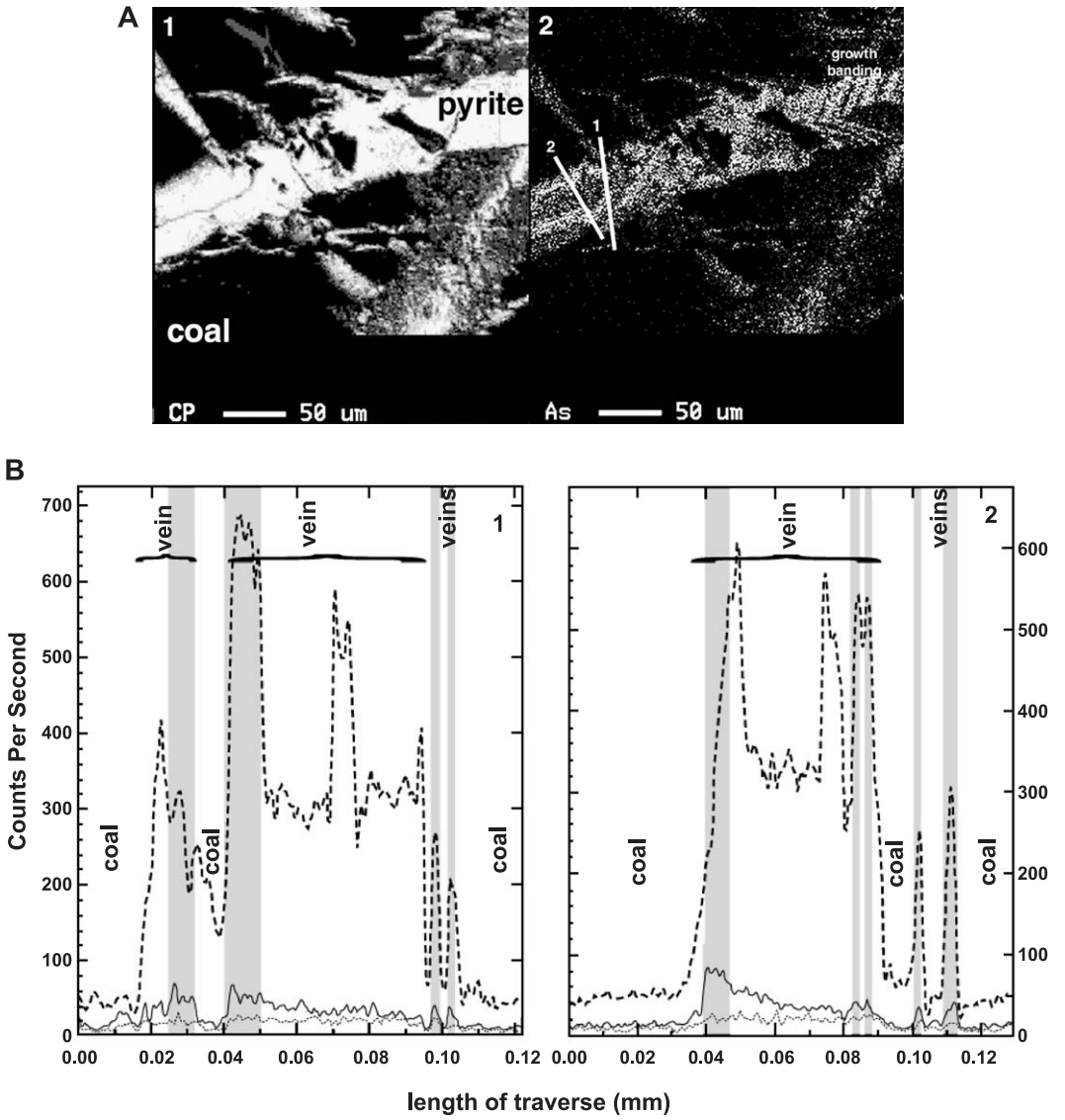

Fig. 5. (A)Photomicrographs of pyrite-filled veins in sample MD-2 from the Kellerman mine showing: (1) Backscatter image of crosscutting pyrite-filled veins in coal; veins are filled with several generations of pyrite; and (2) EPMA As distribution map; As shows enrichment in a multiphase vein (center left of photo; bright gray) and growth banding texture (upper right of photo; bright gray). White lines are the locations of EPMA line scans across the vein; data for As and Hg are displayed in (B). (B) EPMA line scans across multigenerational pyrite-filled fracture (see (A) for location of line scans), showing the concentration profile of Hg (dark solid line) and As (dark dashed line). Bottom dotted line is a background scan. Note that Hg concentration is clearly elevated above background in vein sulfide and fluctuates across the fracture fill, suggesting that the vein is a compound vein composed of multiple generations of pyrite. High Hg concentrations generally correspond to high As concentrations (vertical gray bands). Note also the drop in Hg and As concentration across coal.

Fig. 5A). However, because of the low concentrations of Hg (a maximum of 104 ppm in vein-fill pyrite in Kellerman samples; Table 3), elemental distribution maps did not reveal the distribution of Hg. EPMA X-ray line scans confirmed that Hg content fluctuated across mutigenerational pyrite-filled veins, commonly in concert with As concentration (Fig. 5B). The location of the EPMA line scans are shown in Fig.

5A, and the results are shown in Fig. 5B. In this figure, vertical shaded bars are centered on a subset of the peaks in the Hg line scan. In each case, Hg peaks coincide with elevated As content, and commonly with a distinct As peak. In contrast, there are several As peaks without corresponding Hg peaks. For, example, note the large As peak in the central portion of line scan 1 (Fig. 5B). Also note that As/Hg variability occurs on a distance scale measured in microns. Thus, laser ablation data (25 μm spot size) would not reveal as much of this heterogeneity in the veins as the EPMA element map and line scans with a 2-μm excitation volume. Both As and Hg decrease dramatically in counts/s when the scan crosses coal. Several EPMA line scans across pyrite-filled fractures showed that these elements had elevated concentration at the edge and interior of the fracture fill, suggesting a multigenerational origin (Fig. 5A).

The LA-ICPMS data show that these distinct morphological forms and structural associations of pyrite differ in their relative trace element contents (Fig. 6; Table 3). Mercury is concentrated in the pyrite-filled vein networks associated with folded and faulted coal beds (Fig. 6). In contrast, Hg was at or below detection limits in framboidal pyrite and the pyrite-filled cellular structures in the Lost Creek samples (Fig. 6). Goldhaber et al. (2002, their Fig. 18) illustrate a cluster of low As pyrite framboids infilled by a later generation of As-rich pyrite. There were no "empty" cellular structures observed in the Lost Creek samples. However, cellular structures from Flat Top samples were commonly open or partially filled with minerals. Mercury was detected in pyrite-filled cells from the Flat Top sample, but these cells were crosscut by microfractures and filled by late-stage As-rich pyrite.

Bivariate plots of trace metal contents determined by LA-ICP-MS data extend the bar plots of Fig. 3A and B in that they indicate element associations during the mineralizing process. Specifically, vein-hosted As and Tl have a nearly linear correspondence in both the Kellerman and Flat Top samples (Fig. 7). However,

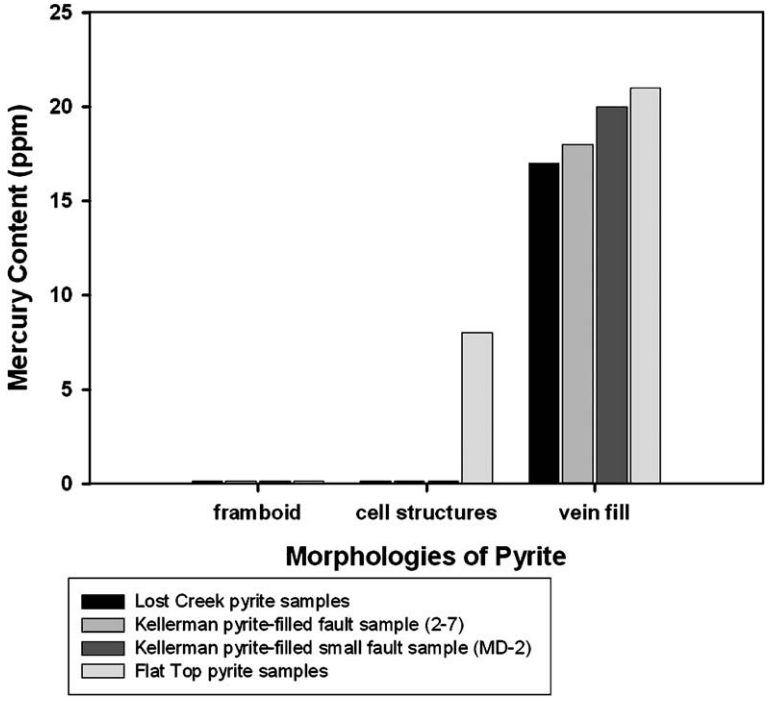

Fig. 6. Plot of Hg contents in framboidal pyrite, massive pyrite in cell structures, and massive pyrite in veins, Warrior field coal samples. Mercury was at or below detection limits in framboidal pyrite (less than 1 ppm). Pyrite-filled cellular structures in the Flat Top mine sample contained Hg because open cell structures, initially filled with calcite or kaolinite that had undergone partial dissolution, were filled by a late-stage pyrite generation. Although the mine sites are widely spaced across the basin, Hg is always concentrated in late-stage vein structures.

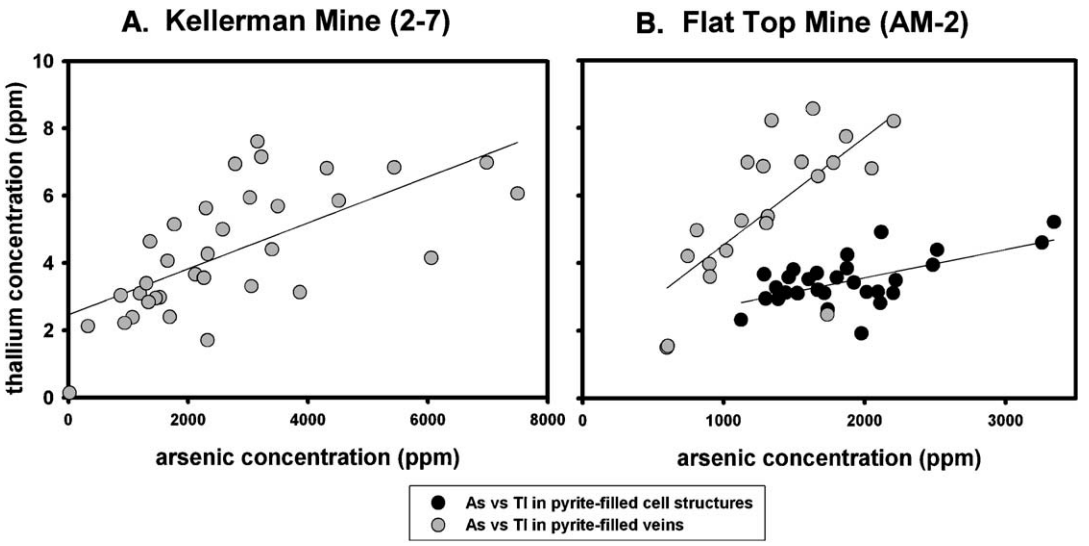

Fig. 7. Plots showing As and Tl content in pyrite-filled structures in coal samples from the Kellerman ($r^2 = 0.44$) and Flat Top ($r^2 = 0.50$ cells; $r^2 = 0.37$ veins) mines. As one element increases in content, the other does also, suggesting that As and Tl are strongly related in source and mode of occurrence.

for the Flat Top sample, the slope is different for trace elements in pyrite-filled cell structures (black circles, Fig. 7) compared to the pyrite-filled veins (gray circles, Fig. 7); the latter is more Tl-rich for a given As content.

Mercury content likewise differs on a relative basis between morphological types of pyrite (Fig. 6). As in the example of As and Tl in Flat Top mine samples, this difference is illustrated in a bivariate plot of Hg versus As and Se (Fig. 8). Mercury and As in pyrite-

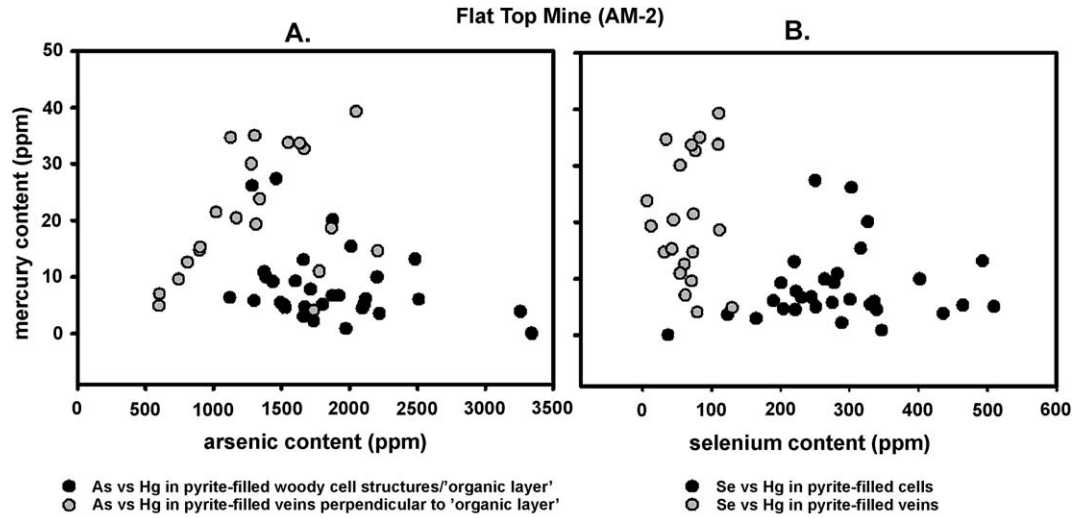

Fig. 8. Plot of As and Hg in pyrite-filled structures, suggesting that there are at least two generations (or populations) of coarse-grained pyrite in coal from the Flat Top mine. Pyrite in veins has higher Hg content than pyrite that fills cellular structures. Overlap in data occurs because the veins and (or) pyrite-filled microfractures crosscut the woody cell structures. (A) Mercury and As plot. (B) Mercury and Se plot. Early cellular-filling pyrite has a low-Hg, high-Se content, whereas the pyrite that fills veins generally has a high-Hg, low-Se content.

filled veins are strongly related, as one element increases in concentration, the other does also (Fig. 8A). In contrast, Hg in pyrite-filled woody cell structures is systematically lower in concentration than in the veins and essentially independent of As content (Fig. 8A). The Hg-versus-Se plots likewise fall into groups as a function of pyrite morphology; vein pyrite is elevated in Hg compared to pyrite-filled cells (Fig. 8B). There is considerable scatter in Fig. 8; because As-rich pyrite in microfractures commonly crosscut cellular structures, either filling the open cells or partially replacing earlier As-poor pyrite, it was sometimes difficult to assign a laser ablation value to a relatively early pyrite phase (cell fill) or late (vein fill).

5.3. Mercury in the coal matrix

Mercury contents in coal are much lower than Hg contents in coarse pyrite (Figs. 3 and 5B). Nonetheless, there is evidence for addition of Hg to coal from mineralizing solutions. Fig. 9 shows a series of point analyses using the LA-ICP-MS along a traverse perpendicular to an As-rich pyrite-filled vein. The transect length is 2 cm (Fig. 9A). The horizontal pyrite-filled vein adjacent to the transect (white bar, Fig. 9A)

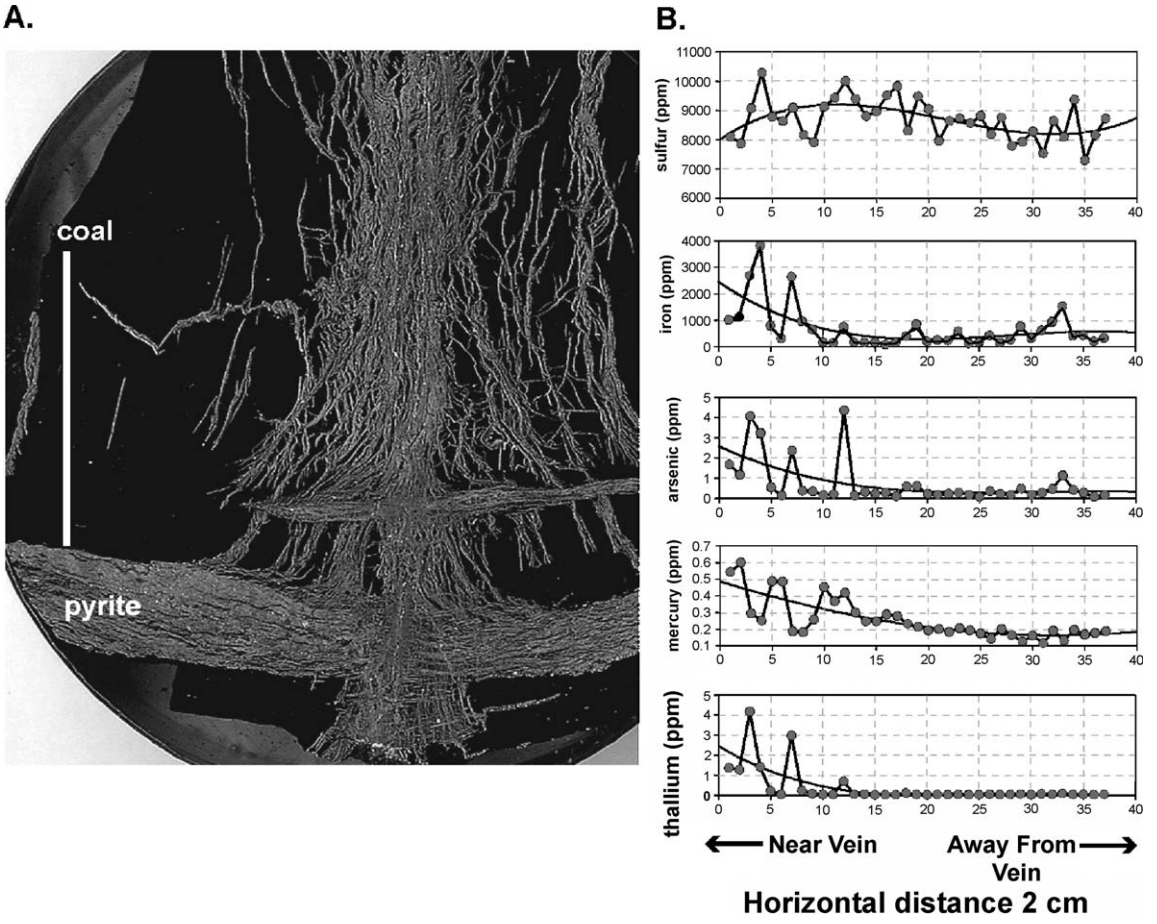

Fig. 9. (A) Sample of coal from the Kellerman mine, showing orthogonal set of pyrite-filled veins. White line is a transect of laser ablation holes in coal, from directly adjacent to As-rich pyrite to a 2-cm distance into the coal. (B) Series of plots showing decrease in element concentrations with increasing distance from As-rich pyrite (near vein = left side of plots). The slight increase in values at 1.8 cm is due to the nearby presence of another trace metal-rich vein.

hosts up to 2600 ppm As. In contrast, the coal immediately adjacent to the pyrite has less than 10-ppm As, and drops to very low values (< 1 ppm As) within about 0.25 cm of the edge of the vein. The coal-hosted As tends to correlate with Fe, suggesting that some of the As is hosted by extremely fine-grained pyrite (Fig. 9B). Thallium correlates with Fe and As, suggesting that the host for Tl is pyrite as well. Mercury is present up to a concentration of 21 ppm in the pyrite, and drops to contents of about 0.8 ppm in directly adjacent coal. In contrast to As and Tl, Hg drops off much more gradually with increasing distance from the edge of the pyrite-filled vein, and is negatively correlated with Fe, As, and Tl. Background Hg values of about 0.15 ppm are reached only at a distance of about 1 cm from the pyrite. Because the Hg content does not correlate with Fe, the Hg host is not pyrite. The trend in Hg values is consistent with diffusion of Hg from vein-filling fluids into adjacent coal. Note also that S remains quite high in coal (>8000 ppm) even where Fe is at low concentration (>200 ppm). This implies that much of the S is present in an organic form.

The control on Hg content of the non-pyrite fraction of coal may be organic S (Skyllberg et al., 2000). The evidence for this statement is in Fig. 10, which shows plots of Hg versus total S in coal from Kellerman and Flat Top mine samples. Iron is not associated with S in these analyses. In both cases, there is a positive correspondence between the two variables, although the absolute abundances differ in the two data sets. The organic Hg content in the Kellerman sample is elevated above median values for coal samples from through out the U.S. (Tewalt et al., 2001), and specifically from the Appalachian basin. Thus, it is likely that there has been a net addition of Hg to the coal matrix.

6. Discussion

Chemical relations between trace elements were investigated by a variety of analytical techniques. Laser ablation analysis showed that trace metals are hosted in pyrite, but the 25-μm beam size did not allow us to precisely determine element zonation and associations. EPMA element distribution maps and line scans with a 2-μm excitation volume demonstrated the heterogeneous nature of the distribution, frequent correlation of the elements Hg and As, and also showed differential element enrichment in a multigenerational vein network. The element distribution map of As in Fig. 4A demonstrates at least two episodes of opening and sealing of the veins by As-poor and an As-rich pyrite.

Based on these results, we conclude that deformation events allowed the introduction of trace metal-rich fluids along faults, veins, and in directly adjacent coal. Tectonism resulted in mega- and microscopic-scale cross cutting pyrite-filled veins with attendant As and Hg assemblages. Earlier cell-filling pyrite and As rich-pyrite overgrowths were likewise associated

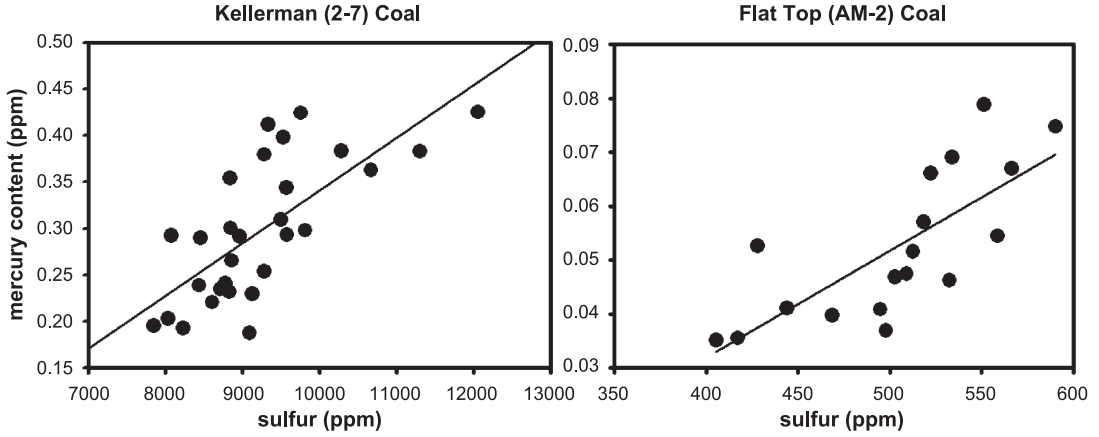

Fig. 10. Plots of Hg and S contents in two coal samples. Mercury contents are strongly correlated with S contents of coal (Kellerman coal, $r^2 = 0.051$; Flat Top coal, $r^2 = 0.57$).

with deformation events. On a macroscopic scale, Hg- and As-rich pyrite is associated with faults related to Alleghanian tectonism (Goldhaber et al., 2002). Coal with early pyrite generations that were Hg- and As-poor, reacted with hydrothermal metal-bearing fluids that were focused along a northwest–southeast trending normal fault system (Goldhaber et al., 2002). These faults formed after significant burial of the coal-bearing units. On the microscopic scale, As-rich pyrite postdates early framboidal pyrite as well as massive pyrite that fills woody cellular structures. Thus, framboidal and massive cell-filling pyrite are likely early diagenetic phases. In contrast, As- and Hg-rich pyrite commonly occurs as overgrowths on the earlier generations of pyrite and as a late-stage vein-filling mineral. We interpret the positively correlated As and Tl vein data in Fig. 6 to indicate that the two elements were added from the same fluid, whereas the data from late pyrite associated with pyrite-filled cell structures suggest the existence of a separate As-rich, Tl-poor mineralizing fluid. Likewise, Hg-rich pyrite is characteristically As-rich, but an As-rich Hg-poor pyrite was also recognized.

Mercury and As are most likely in solid solution with pyrite. LA-ICPMS data suggest that Se may also occur as solid solution in pyrite because Se contents commonly shows a positive correlation with As and Hg in the vein networks (Fig. 8). For example, in samples collected from the fault zone in the Kellerman mine, high Se concentrations (up to 590 ppm) corresponded to high Hg concentrations (up to 104 ppm). However, in pyrite samples from the Flat Top mine, the highest Se contents were found in early massive pyrite that filled cellular structures (avg. 286 ppm), not in later vein-filling pyrite (66 ppm); whereas, the Hg contents in the cellular structures were low (avg. 8 ppm), and high in the vein-filling pyrite (avg. 21 ppm) (Table 3).

Although As-rich pyrite is the dominant residence for Hg, our data also suggest that Hg has been added epigenetically to the coal matrix. This is most clearly seen in the LA-ICP-MS data of Fig. 9B. In the figure, the decrease of Hg away from the pyrite vein edge implies diffusion of Hg into the coal matrix. The Hg in coal occurs against a background of very-low Fe values (i.e., low pyrite), but elevated S content. This elevated non-pyrite S (i.e., organic S) may be significant. Fig. 10 documents a positive correlation between Hg and non-pyrite S in both the Kellerman and Flat Top Mines. The abundance of Hg is significantly greater in the Kellerman mine data, which has greater than an order-of-magnitude higher S content than does the Flat Top mine results.

It is likely that this Hg–S correlation reflects uptake of Hg by organic S compounds in the coal. The binding of Hg by organic S compounds is well documented (Skyllberg et al., 2000). Specifically, Hg has a very high affinity for thiol (RSH) and other reduced S groups (Xia et al., 1999). Organic S is a very common constituent of coal, particularly coal formed in a marginal marine setting. This leads us to hypothesize that organic S may have been an early diagenetic constituent of the coal and it acted to trap Hg, which was added during later epigenesis.

The mechanism for trapping Hg and associated trace elements in pyrite is presently not well characterized, but likely involves either addition of Fe or S to a hydrothermal solution passing through the coal. As discussed in more detail in Goldhaber et al. (2002), the fluids, which introduced As to Black Warrior Basin coals, were likely H_2S-bearing. This is because complexation with bisulfide ion (HS^-) is the dominant mechanism for transport of As and associated trace elements in hydrothermal fluids. To precipitate the As-and Hg-rich pyrite, one potential pathway is to add Fe to this H_2Sbearing fluid. Iron addition through dissolution of Fe-bearing carbonate minerals (Eq. (1)) is a dominant process in forming the 'CarlinType' Au deposits (Hofstra and Cline, 2000).

$$2H_2S + FeCO_3 = FES_2 + H_2 + H_2CO_3 \quad (1)$$

In these Carlin-Type deposits, As-rich pyrite is the major residence for Au, and the suite of elements contained in pyrite is nearly identical to that documented in Warrior coal field pyrite. This mechanism for pyrite precipitation in coal from hydrothermal fluids is likely because siderite ($FeCO_3$) is commonly associated with coal beds (e.g. Stach et al., 1982, p. 293).

A second mechanism for precipitation of As-rich pyrite is addition of an increment of H_2S to a solution at or near saturation with pyrite. A mechanism for this H_2S addition is thermal decomposition of organic S in the coal. Release of thermally labile organically bound H_2S (Tissot and Welte, 1984) has been shown to

precipitate metallic sulfides in Illinois coal beds (Whelan et al., 1988). Furthermore, S-rich (including organic S-rich) coals correlate spatially with As abundance in the Black Warrior Basin, suggesting a potential link between organic S and As-rich pyrite abundance.

7. Conclusions

Mercury in the Warrior field coals of northwestern Alabama is primarily hosted in late-stage post-coalification pyrite that occurs as overgrowths on woody cellular structures and in pyrite-filled veins and faults. Elevated contents of Hg, As, Tl, and other trace metals in pyrite occurred during a late-stage metal-bearing fluid migration event, probably related to Alleghanian tectonism. Because the trace metals exhibit similar modes of distribution and enrichment in the pyrite, the metals are presumed to originate from the same fluid source.

Trace-metal rich pyrite in Warrior field coal tends to be coarse-grained, and therefore, amenable to removal by coal-cleaning procedures. However, sulfide-rich wastes from the cleaning processes would then concentrate the potentially toxic elements. Mercury, As, and Tl are present in Warrior field mineralized coal at high enough concentrations to pose possible hazards, even after pyrite removal. In some samples studied here, Hg has penetrated into the coal matrix. The geographic extent of the process has not been characterized, but it is likely to be limited to structurally disrupted areas with very high As and Hg.

Acknowledgements

The Minerals, Crustal Imaging and Characterization, and the Energy Resources Programs of the U.S. Geological Survey funded this study. Jack C. Pashin, Alabama Geological Survey, provided valuable field assistance. Amy Bern at the U.S. Geological Survey Denver Microbeam Laboratory ran EPMA element maps and line scans. Trace metal analyses were obtained with the assistance of Tracy L. Copp, U.S. Geological Survey Laser Ablation ICP-MS Laboratory, Denver, CO.

References

Affolter, R.H., Hatch, J.R., 2002. Characterization of the quality of coals from the Illinois Basin, Chapter E. In: Hatch, J.R., Affolter, R.H. (Eds.), Resource Assessment of the Springfield, Herrin, Danville, and Baker Coals in the Illinois Basin. U.S. Geological Survey Professional Paper, 1625-D, pp. E1–E222.

Bragg, L.J., Oman, J.K., Tewalt, S.J., Oman, C.L., Rega, N.H., Washington, P.M., Finkelman, R.B., 1997. U.S. Geological Survey Coal Quality (COALQUAL) database; version 2.0, U.S.

Culbertson, W.C., 1964. Geology and coal resources of the coal-bearing rocks of Alabama. U.S. Geological Survey Bulletin. 1182-B, B1–B79.

Diehl, S.F., Goldhaber, M.B., Hatch, J.R., Kolker, A., Pashin, J.C., Koenig, A.E., 2002. Mineralogic residence and sequence of emplacement of arsenic and other trace elements in coals of the Warrior Basin, Alabama. 19th International Pittsburgh Coal Conference, University of Pittsburgh, Pittsburgh, PA. CD-ROM 14 pp.

Diehl, S.F., Smith, K.S., Desborough, G.A., Goldhaber, M.B., 2003. Trace-metal sources and their release from mine wastes; Examples from humidity cell tests of hard-rock mine waste and from Warrior Basin coal. In: Barnhisel, R.I. (Ed.), Working Together for Innovative Reclamation: Proceedings of a Joint Conference of the 9th Billings Land Reclamation Symposium and the 20th Annual Meetings of the American Society of Mining and Reclamation, Lexington, KY. CD-ROM, pp. 232–253.

Environmental Protection Agency (EPA), 1997. Mercury Study; Report to Congress, Volume II: An Inventory of Anthropogenic Mercury Emissions in the U.S., EPA-452/R-97-004 (online at http://www.ega.gov/ttn/oarpg/t3/reports/volume2.pdf).

Finkelman, R.B., Orem, W., Castranova, V., Tatu, C.A., Belkin, H.E., Zheng, B., Lerch, H.E., Maharaj, S.V., Bates, A.L., 2002. Health impacts of coal and coal use; possible solutions. International Journal of Coal Geology 50, 425–443.

Goldhaber, M.B., Hatch, J.R., Pashin, J.C., Offield, T.W., Finkelman, R.B., 1997. Anomalous arsenic and fluorine concentrations in Carboniferous coal, Black Warrior Basin, Alabama; evidence for fluid expulsion during Alleghanian thrusting? Annual Meeting-Geological Society of America 29 (6), A51.

Goldhaber, M.B., Bigelow, R.C., Hatch, J.R., Pashin, J.C., 2000. Distribution of a suite of elements including arsenic and mercury in Alabama coal. U.S. Geological Survey Miscellaneous Field Study Map MF-233.

Goldhaber, M.B., Lee, R.C., Hatch, J.R., Pashin, J.C., Treworgy, J., 2002. The role of large-scale fluid flow in subsurface arsenic enrichment. In: Welch, A., Stollenwerk, K. (Eds.), Arsenic in Ground Water: Occurrence and Geochemistry, vol. 5. Kluwer Academic Publishing, Boston, MA, pp. 127–176.

Hatch, J.R., Goldhaber, M.B., Pashin, J.C., 2001. Anomalous arsenic contents in Lower Pennsylvanian coals, warrior field, Northwestern Alabama, USA. In: Sakkestad, B.A. (Ed.), The Proceedings of the 26th International Technical Conference on Coal Utilization and Fuel Systems, Gaithersburg, MD, pp. 659–667.

Hofstra, A.H., Cline, J.S., 2000. Characteristics and models for

Carlin-type gold deposits. Reviews in Economic Geology 13, 163–220.

Huggins, F.E., 2002. Overview of analytical methods for inorganic constituents in coal. International Journal of Coal Geology 50, 169–214.

Kolker, A., Goldhaber, M.B., Hatch, J.R., Meeker, G.P., Koeppen, R.P., 1999. Arsenic-rich pyrite in coals of the warrior field, northwestern Alabama: Mineralogical evidence for a hydrothermal origin. Abstracts with Programs, Geological Society of America 31 (7), A402.

Oman, C.L., Finkelman, R.B., Halili, N., Goldhaber, M.B., 1995. Anomalous trace element concentrations in coal from the Warrior Basin, Alabama. Abstracts with Programs—Southeastern Section, Geological Society of America 27 (2), A78.

Pashin, J.C., 1991. Regional analysis of the Black Creek-Cobb coalbed methane target interval, Black Warrior Basin, Alabama. Bulletin-Geological Survey of Alabama 145 (127 pp).

Pashin, J.C., Carroll, R.E., Hatch, J.R., Goldhaber, M.B., 1999. Mechanical and thermal control of cleating and shearing in coal: examples from the Alabama coalbed methane fields, USA. In: Mastalerz, M., Glickson, M., Golding, S. (Eds.), Coalbed Methane: Scientific, Environmental and Economic Evaluation. Kluwer Academic Publishing, Dordrecht, pp. 305–327.

Ridley, W.I., 2000. Instruction manual for "Quantlaser"; a batch process macro for reduction of quantitative laser ablation data. Open-File Report-U.S. Geological Survey 00-0311 (42 pp).

Sakulpitakphon, T., Hower, J.C., Schram, W.H., Ward, C.R., 2004. Tracking mercury from the mine to the power plant: geochemistry of the Manchester coal bed, Clay County, Kentucky. International Journal of Coal Geology 57, 127–141.

Skyllberg, U., Xia, K., Bloom, P.R., Nater, E.A., Bleam, W.F., 2000. Binding of mercury (II) to reduced S in soil organic matter along upland-peat soil transects. Journal of Environmental Quality 29, 855–865.

Smith, S., 2001. Reformatted data from the National Uranium Resource Evaluation (NURE) Hydrogeochemical and Stream Sediment Reconnaissance (HSSR) Program http://pubs.usgs.gov/of/1997/ofr-97-0492/.

Stach, E., Mackowsky, M.-Th., Teichmüller, M., Taylor, G.H., Chandra, D., Teichmüller, R., 1982. Stach's Textbook of Coal Petrology. Gebrüeder Borntraeger, Berlin, p. 535.

Tewalt, S.J., Bragg, L.J., Finkelman, R., 2001. Mercury in U.S. coal; abundance, distribution, and modes of occurrence. Fact Sheet, U.S. Geological Survey, Report: FS 0095-01, 4 pp. (online at http://pubs.usgs.gov/factsheet/fs095-01).

Tissot, B.P., Welte, D.H., 1984. Petroleum Formation and Occurrence. Springer-Verlag, Berlin, p. 538.

Vassilev, S.V., Tascón, J.M.D., 2003. Methods for Characterization of inorganic and mineral matter in coal: a critical overview. Energy and Fuels 17, 271–281.

Ward, C.R., 2002. Analysis and significance of mineral matter in coal seams. International Journal of Coal Geology 50, 135–168.

Whelan, J.F., Cobb, J.C., Rye, R.O., 1988. Stable isotope geochemistry of sphalerite and other mineral matter in coal beds of the Illinois and Forest City basins. Economic Geology 83, 990–1007.

Wilson, S.A., Ridley, W.I., Koenig, A.E., 2002. Development of sulfide calibration standards for the laser ablation inductively-coupled plasma mass spectrometry technique. Journal of Analytical Atomic Spectrometry 17, 405–409.

Xia, K., Skyllberg, U.L., Bleam, W.F., Bloom, P.R., Nater, E.A., Helmke, P.A., 1999. X-ray absorption spectroscopic evidence for the complexation of Hg(II) by reduced sulfur in soil humic substances. Environmental Science Technology 33, 257–261.